

Effects of jet quenching on high p_T hadron spectra in high-energy nuclear collisions

Xin-Nian Wang

*Nuclear Science Division, Mailstop 70A-3307, Lawrence Berkeley National Laboratory, Berkeley, California 94720
and Institute for Nuclear Theory, University of Washington, Seattle, Washington 98195-1550*

(Received 22 April 1998)

Since large- p_T particles in high-energy hadronic or nuclear collisions come from jet fragmentation, jet quenching due to parton energy loss in dense matter will cause the suppression of large- p_T hadron spectra in high-energy heavy-ion collisions. Assuming an effective energy loss dE/dx for the high- E_T partons, effective jet fragmentation functions are constructed in which leading hadrons will be suppressed. Using such effective fragmentation functions, high- p_T hadron spectra and particle suppression factors relative to pp collisions are estimated in central high-energy nuclear collisions with a given range of the assumed dE/dx . It is found that the suppression factors are very sensitive to the value of the effective energy loss. Systematic nuclear and flavor dependence of the hadron spectra are also studied. [S0556-2813(98)03610-3]

PACS number(s): 25.75.-q, 12.38.Mh, 13.87.-a, 24.85.+p

I. INTRODUCTION

An ideal quark-gluon plasma (QGP) has often been defined as a system of weakly interacting quarks and gluons in both thermal and chemical equilibrium. However, recent theoretical investigations based on a perturbative QCD-inspired model [1,2] show that it is increasingly difficult for the initially produced partons to evolve into thermal equilibrium, let alone chemical equilibrium. Therefore, one might have a generalized QGP simply as an interacting and deconfined parton system with a *large size* and *long lifetime*.

One can find many examples of an interacting parton system in collisions involving strong interaction. But so far none of them can be considered a QGP in terms of either the ideal or generalized definition. At a distance much smaller than the confinement scale Λ_{QCD} and normally in the earliest time of the collision, the interaction can be described by perturbative QCD (pQCD). Later on, the produced partons will then combine with each other via nonperturbative interactions and finally hadronize into hadrons. Therefore, one can consider that there exists an interacting parton system during the prehadronization stage in, e.g., e^+e^- annihilation and deeply inelastic e^-p processes, which is, however, limited only to a space-time region characterized by the confinement scale Λ_{QCD} . The characteristic particle spectrum (in p_T and rapidity) and the ratios of produced particles are then determined by the physics of pQCD and nonperturbative hadronization. In ultrarelativistic heavy-ion collisions, one seeks to produce a similar interacting parton system but at a much larger scale of the order of a nucleus size and for a long period of time (e.g., a QGP). Therefore, one should study those experimental observables which are unique to the large size and long lifetime of an interacting partonic system as signals of a quark-gluon plasma.

Among many proposed signals of a quark-gluon plasma [3], hard probes associated with hard processes are especially useful because they are produced in the earliest stage of the collision and their abilities to probe the dense matter are less complicated by the hadronization physics. The merits of hard probes are even more apparent at high energies because those processes also dominate the underlying collision dy-

namics which will determine the initial conditions of the produced partonic system [4,2]. Study of them will then enable us to probe the early parton dynamics and the evolution of the quark-gluon plasma.

In general, one can divide the hard probes into two categories: thermal emission and particle suppression by the medium. Particle production, like photon/dilepton and charm particles, from thermal emission can be considered as thermometers of the dense medium. Their background comes from the direct production in the initial collision processes. On the other hand, suppression of particles produced in the initial hard processes, like high- p_T particles from jets and J/Ψ , can reveal evidence of the parton energy loss in dense matter and the deconfinement of the partonic system. Thermal production of these particles is expected to be negligible. Therefore, in both cases, one needs to know the initial production rate accurately enough. Another advantage of these hard probes is that the initial production rate can be calculated via pQCD, especially if we understand the modest nuclear modification one would expect to happen.

In this paper, we will discuss high- p_T particles as probes of the dense matter since one expects high- E_T partons which produce these high- p_T particles will interact with the dense medium and lose energy. Medium-induced energy loss of a high-energy parton traversing a dense QCD medium is interesting because it depends sensitively on the density of the medium and thus can be used as a probe of the dense matter formed in ultrarelativistic heavy-ion collisions. As recent studies demonstrated [5–7], it is very important to take into account the coherent effect in the calculation of radiation spectrum induced by multiple scattering of a fast parton. The so-called Landau-Pomeranchuk-Migdal effect can lead to very interesting, and sometimes nonintuitive results for the energy loss of a fast parton in a QCD medium. Another feature of the induced energy loss is that it depends on the parton density of the medium via the final transverse momentum broadening that the parton receives during its propagation through the medium. One can therefore determine the parton density of the produced dense matter by measuring the energy loss of a fast parton when it propagates through the medium.

Unlike in the QED case, where one can measure directly the radiative energy loss of a fast electron, one cannot measure directly the energy loss of a fast leading parton in QCD. Since a parton is normally studied via a jet, a cluster of hadrons in the phase space, an identified jet can contain particles both from the fragmentation of the leading parton and from the radiated partons. If we neglect the p_T broadening effect, the total energy of the jet should not change even if the leading parton suffers radiative energy loss. What should be changed by the energy loss are the particle distributions inside the jet or the fragmentation functions and the jet profile. Therefore, one can only measure parton energy loss indirectly via the modification of the jet fragmentation functions and jet profile. For this purpose, it was recently proposed [8,9] that the jet quenching can be studied by measuring the p_T distribution of charged hadrons in the opposite direction of a tagged direct photon. Since a direct photon in the central rapidity region ($y=0$) is always accompanied by a jet in the opposite transverse direction with roughly equal transverse energy, the p_T distribution of charged hadrons in the opposite direction of the tagged direct photon is directly related to the jet fragmentation functions with known initial energy. One can thus directly measure the modification of the jet fragmentation and then determine the energy loss suffered by the leading parton with given initial energy.

Similarly, the single-particle spectrum can also be used to study the effect of parton energy loss as proposed in Ref. [10], since the suppression of large- E_T jets naturally leads to the suppression of large- p_T particles. However, since the single-particle spectrum is a convolution of the jet cross section and jet fragmentation function, the suppression of produced particles with a given p_T results from jet quenching with a range of initial transverse energies. Therefore, one cannot measure the modification of the jet fragmentation function or the energy loss of a jet with known initial transverse energy from the single-particle p_T spectrum as precisely as in the case of tagged direct photons. One clear advantage of the single inclusive particle spectrum is the large production rate of moderately high- p_T particles, while the production rate of large- p_T direct photons is relatively much smaller at the designed luminosity of the relativistic heavy-ion collider (RHIC) [9]. Therefore, with much less experimental effort, one can still study qualitatively the effect of jet quenching and extract the average value of the parton energy loss from single-particle spectra at high p_T .

In this paper, we will conduct a systematic study of the effects of parton energy loss on single-particle transverse momentum spectra in central $A+A$ collisions in the framework of modified effective jet fragmentation functions. We study within this framework the dependence of the spectra on the effective parton energy loss. We will discuss the energy or p_T and A dependence of the energy loss and jet quenching. Finally, flavor dependence of the spectra will also be discussed.

II. MODIFIED JET FRAGMENTATION FUNCTIONS

Jet fragmentation functions have been studied extensively in e^+e^- , ep , and $p\bar{p}$ collisions [11]. These functions describe the particle distributions in the fractional energy, $z = E_h/E_{\text{jet}}$, in the direction of a jet. The measured depen-

dence of the fragmentation functions on the momentum scale is shown to satisfy the QCD evolution equations very well. We will use the parametrizations of the most recent analysis [12,13] in both z and Q^2 for jet fragmentation functions $D_{h/a}^0(z, Q^2)$ to describe jet (a) fragmentation into hadrons (h) in the vacuum.

In principle, one should study the modification of jet fragmentation functions in a perturbative QCD calculation in which induced radiation of a propagating parton in a medium and Landau-Pomeranchuk-Migdal interference effect can be dynamically taken into account. However, for the purpose of our current study, we can use a phenomenological model to describe the modification of the jet fragmentation function due to an effective energy loss dE/dx of the parton. In this model we assume: (1) A quark-gluon plasma is formed with a transverse size of the colliding nuclei, R_A . A parton with a reduced energy will only hadronize outside the deconfined phase and the fragmentation can be described as in e^+e^- collisions. (2) The mean free path of inelastic scattering for the parton a inside the QGP is λ_a which we will keep a constant throughout this paper. The radiative energy loss per scattering is ϵ_a . The energy loss per unit distance is thus $dE_a/dx = \epsilon_a/\lambda_a$.

The probability for a parton to scatter n times within a distance ΔL is given by a Poisson distribution,

$$P_a(n, \Delta L) = \frac{(\Delta L/\lambda_a)^n}{n!} e^{-\Delta L/\lambda_a}. \quad (1)$$

We also assume that the mean free path of a gluon is half that of a quark, and the energy loss dE/dx is twice that of a quark. (3) The emitted gluons, each carrying energy ϵ_a on the average, will also hadronize according to the fragmentation function with the minimum scale $Q_0^2 = 2.0 \text{ GeV}^2$. We will also neglect the energy fluctuation given by the radiation spectrum for the emitted gluons. Since the emitted gluons only produce hadrons with very small fractional energy, the final modified fragmentation functions in the moderately large z region are not very sensitive to the actual radiation spectrum and the scale dependence of the fragmentation functions for the emitted gluons.

This is definitely a simplified picture. In a more realistic scenario, one should also consider both the longitudinal and transverse expansion. Because of the expansion, the actual parton energy loss will change as it propagates through the evolving system resulting in a different total energy loss as recently studied in Ref. [14]. Since we are mostly interested in the overall effects, we can neglect the details of the evolution history and concentrate on the modification of high- p_T hadron spectra due to an assumed total energy loss or averaged energy loss dE/dx per unit distance. It might require much more elaborated study to find out the effects of the dependence of the energy loss on the dynamical evolution of the system. It is beyond the scope of this paper.

We will consider the central rapidity region of high-energy heavy-ion collisions. We assume that a parton with initial transverse energy E_T will travel in the transverse direction in a cylindrical system. With the above assumptions, the modified fragmentation functions for a parton traveling a distance ΔL can be approximated as

$$D_{h/a}(z, Q^2, \Delta L) = \frac{1}{C_N^a} \sum_{n=0}^N P_a(n, \Delta L) \frac{z_n^a}{z} D_{h/a}^0(z_n^a, Q^2) + \langle n_a \rangle \frac{z'_a}{z} D_{h/g}^0(z'_a, Q_0^2), \quad (2)$$

where $z_n^a = z/(1 - n\epsilon_a/E_T)$, $z'_a = zE_T/\epsilon_a$, and $C_N^a = \sum_{n=0}^N P_a(n)$. We limit the number of inelastic scattering to $N = E_T/\epsilon_a$ by energy conservation. For large values of N , the average number of scattering within a distance ΔL is approximately $\langle n_a \rangle \approx \Delta L/\lambda_a$. The first term corresponds to the fragmentation of the leading partons with reduced energy $E_T - n\epsilon_a$ and the second term comes from the emitted gluons each having energy ϵ_a on the average. Detailed discussion of this modified effective fragmentation function and its limitations can be found in Ref. [9].

III. ENERGY LOSS AND SINGLE-PARTICLE p_T SPECTRUM

To calculate the p_T distribution of particles from jet fragmentation in pp and the central heavy-ion collision, one simply convolutes the fragmentation functions with the jet cross sections [15],

$$\frac{d\sigma_{\text{hard}}^{pp}}{dy d^2p_T} = K \sum_{abcdh} \int_{x_{a \min}}^1 dx_a \int_{x_{b \min}}^1 dx_b f_{a/p}(x_a, Q^2) \times f_{b/p}(x_b, Q^2) \times \frac{D_{h/c}^0(z_c, Q^2)}{\pi z_c} \frac{d\sigma}{d\hat{t}}(ab \rightarrow cd), \quad (3)$$

for pp and

$$\frac{dN_{\text{hard}}^{AA}}{dy d^2p_T} = K \int d^2r t_A^2(r) \sum_{abcdh} \int_{x_{a \min}}^1 dx_a \int_{x_{b \min}}^1 dx_b f_{a/A}(x_a, Q^2, r) \times f_{b/A}(x_b, Q^2, r) \times \frac{D_{h/c}(z_c, Q^2, \Delta L)}{\pi z_c} \frac{d\sigma}{d\hat{t}}(ab \rightarrow cd), \quad (4)$$

for AA collisions, where $z_c = x_T(e^y/x_a + e^{-y}/x_b)/2$, $x_{b \min} = x_a x_T e^{-y}/(2x_a - x_T e^y)$, $x_{a \min} = x_T e^y/(2 - x_T e^{-y})$, and $x_T = 2p_T/\sqrt{s}$. The nuclear thickness function is normalized to $\int d^2r t_A(r) = A$. The $K \approx 2$ factor accounts for higher-order corrections [16]. The parton distributions per nucleon in a nucleus (with atomic mass number A and charge number Z),

$$f_{a/A}(x, Q^2, r) = S_{a/A}(x, r) \times \left[\frac{Z}{A} f_{a/p}(x, Q^2) + \left(1 - \frac{Z}{A} \right) f_{a/n}(x, Q^2) \right], \quad (5)$$

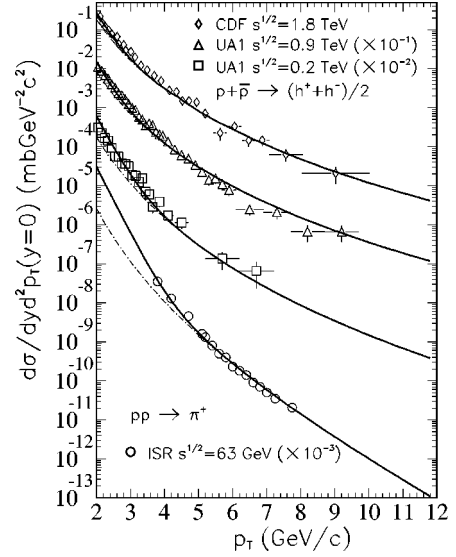


FIG. 1. The charged particle p_T spectra in pp and $p\bar{p}$ collisions. The dot-dashed lines are from jet fragmentation only and solid lines include also soft production parametrized in an exponential form. The experimental data are from Refs. [20–23].

are assumed to be factorizable into parton distributions in a nucleon $f_{a/N}(x, Q^2)$ and the parton shadowing factor $S_{a/A}(x, r)$ which we take the parametrization used in the HIJING model [17]. Neglecting the transverse expansion, the transverse distance a parton produced at (r, ϕ) will travel is $\Delta L(r, \phi) = \sqrt{R_A^2 - r^2(1 - \cos^2 \phi)} - r \cos \phi$.

In principle, one should also take into account the intrinsic transverse momentum and the transverse momentum broadening due to initial multiple scattering. These effects (so-called Cronin effects) are found to be very important to the final hadron spectra at around superproton synchrotron (SPS) energies ($\sqrt{s} = 20\text{--}50$ GeV) [18]. However, at RHIC energy which we are discussing in this paper, one can neglect them (about 10–30% correction) to a good approximation.

We will use the Martin-Roberts-Stirling (MRS) $D - t$ parametrization of the parton distributions [19] in a nucleon. The resultant p_T spectra of charged hadrons (π^\pm, K^\pm) for pp and $p\bar{p}$ collisions are shown in Fig. 1 together with the experimental data [20–23] for $\sqrt{s} = 63, 200, 900,$ and 1800 GeV. The calculations (dot-dashed line) from Eq. (3) with the jet fragmentation functions given by Refs. [12,13] agree with the experimental data remarkably well, especially at large p_T . However, the calculations are consistently below the experimental data at low p_T , where we believe particle production from soft processes, like string fragmentation of the remanent colliding hadrons, becomes very important. To account for particle production at smaller p_T , we introduce a soft component to the particle spectra in an exponential form,

$$\frac{dN_{\text{soft}}^{pp}}{dy d^2p_T} = C e^{-p_T/T}, \quad (6)$$

with a parameter $T = 0.25$ GeV/c. This exponential form is a reasonable fit to the data of hadron p_T spectra of $p\bar{p}$ collisions at $\sqrt{s} = 200$ GeV below $p_T < 2$ GeV/c. The fit is not very good below $p_T = 0.5$ GeV and the parameter T should

TABLE I. Charged hadron rapidity density and inelastic cross sections for pp collisions at different colliding energies from HIJING calculations.

| \sqrt{s} (GeV) | 63 | 200 | 900 | 1800 |
|-------------------------|-----|-----|-----|------|
| dN^{pp}/dy | 1.9 | 2.4 | 3.2 | 4.0 |
| σ_{in}^{pp} (mb) | 35 | 44 | 50 | 58 |

also depend on colliding energy \sqrt{s} . However, for a rough estimate of the spectra at low p_T this will be enough and we will keep T a constant.

The normalization in Eq. (6) is determined from the charged hadron rapidity density in the central region:

$$C = \frac{1}{2\pi T^2} \left(\frac{dN^{pp}}{dy} - \frac{dN_{hard}^{pp}}{dy} \right), \quad (7)$$

where

$$\frac{dN_{hard}^{pp}}{dy} = \frac{1}{\sigma_{in}^{pp}} \int d^2p_T \frac{d\sigma_{hard}^{pp}}{dy d^2p_T}. \quad (8)$$

Table I lists the values of the charged hadron rapidity density and the inelastic cross sections of pp collisions from HIJING calculations which we will use to determine the normalization in Eq. (6) at different energies.

The total p_T spectrum for charged hadrons in pp collisions including both soft and hard components is then

$$\frac{dN^{pp}}{dy d^2p_T} = \frac{dN_{soft}^{pp}}{dy d^2p_T} + \frac{1}{\sigma_{in}^{pp}} \frac{d\sigma_{hard}^{pp}}{dy d^2p_T}, \quad (9)$$

which are shown in Fig. 1 as solid lines. As one can see it improves the agreement with data at lower transverse momentum.

We now also assume that the charged multiplicity from soft particle production is proportional to the total number of wounded nucleons in AA collisions which scales like A , while the production from hard processes is proportional to the number of binary nucleon-nucleon collisions which scales like $A^{4/3}$. At low p_T both types of processes contribute to the particle spectrum. Therefore the A scaling of the spectrum at low p_T depends on the interplay of soft and hard processes. In the HIJING model [17] with a cutoff of $E_{T0} = 2$ GeV for jet production the low- p_T spectra scale like $A^{1.1}$. To take into account of the uncertainty due to the interplay between soft and hard processes, we assume the hadron spectrum in central AA collisions is

$$\frac{dN^{AA}}{dy d^2p_T} = A^{\alpha_h} \frac{dN_{soft}^{pp}}{dy d^2p_T} + \frac{dN_{hard}^{AA}}{dy d^2p_T}, \quad (10)$$

where $\alpha_h = 1.0-1.1$.

To calculate $dN_{hard}^{AA}/dy d^2p_T$, we will take into account both the effect of nuclear shadowing on parton distributions and the modification of the jet fragmentation functions due to parton energy loss inside a medium. From Eq. (4) we see that it will be proportional to an overlap function of central AA collisions $T_{AA}(0)$. In a hard-sphere model for nuclear distribution, $T_{AA}(0) = 9A^2/8\pi R_A^2$ and $R_A = 1.2A^{1/3}$ fm.

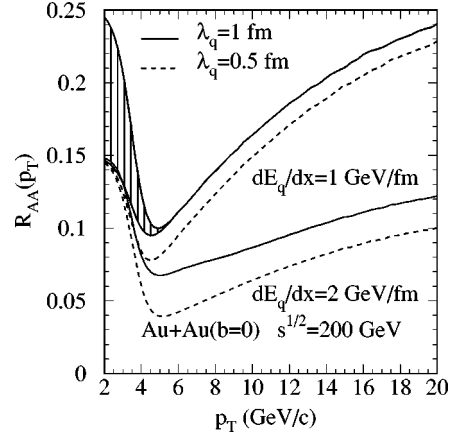


FIG. 2. The suppression factor or ratio of charged particle p_T spectrum in central Au+Au over that of pp collisions at $\sqrt{s} = 200$ GeV, normalized by the total binary nucleon-nucleon collisions in central Au+Au collisions, with different values of the energy loss dE_q/dx and the mean free path λ_q of a quark inside the dense medium, the shaded area indicates the uncertainty of the effective A scaling of low- p_T spectra depending on the interplay of soft and hard processes

We now define an effective suppression factor, or the ratio,

$$R_{AA}(p_T) = \frac{dN_{AA}/dy/d^2p_T}{\sigma_{in}^{pp} T_{AA}(0) dN_{pp}/dy/d^2p_T}, \quad (11)$$

between the spectrum in central AA and pp collisions which is normalized to the effective total number of binary NN collisions in a central AA collision. If none of the nuclear effects (shadowing and jet quenching) are taken into account, this ratio should be unity at large transverse momentum. Shown in Fig. 2 are the results for central Au+Au collisions at the RHIC energy with $dE_q/dx = 1, 2$ GeV/fm, and $\lambda_q = 1$ (solid), 0.5 fm (dashed), respectively. As we have argued before, jet energy loss will result in the suppression of high p_T particles as compared to pp collisions. Therefore, the ratio at large p_T in Fig. 2 is smaller than one due to the energy loss suffered by the jet partons. It, however, increases with p_T because of the constant energy loss we have assumed here. At hypothetically large p_T when the total energy loss is negligible compared to the initial jet energy, the ratio should approach to one.

Since there is always a coronal region with an average length of λ_q in the system where the produced parton jets will escape without scattering or energy loss, the suppression factor can never be infinitely small. For the same reason, the suppression factor also depends on the parton's mean free path, λ_q . It is thus difficult to extract information on both dE_q/dx and λ_q simultaneously from the measured spectra in a model independent way.

At small p_T , particles from soft processes (or from hadronization of QGP) dominate. The ratio $R_{AA}(p_T)$ is then very sensitive to the A -scaling behavior of the soft particle production. Since we assumed an effective scaling, A^{α_h} with $\alpha_h = 1.0-1.1$, for the low- p_T particle production, the ratio should approach $A^{\alpha_h}/\sigma_{pp} T_{AA}(0) = 0.149-0.253$ at small p_T for central Au+Au collisions at the RHIC energy, as shown

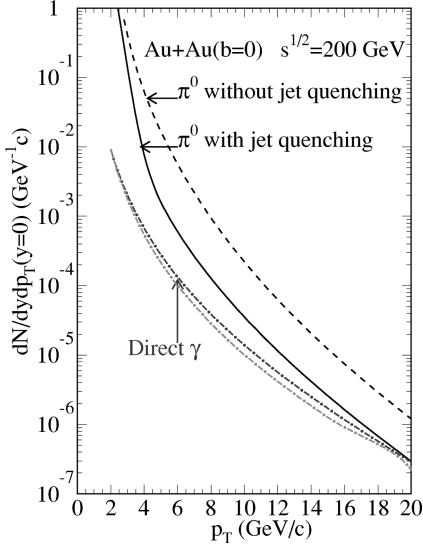


FIG. 3. The inclusive p_T distribution for π^0 with (solid) and without (dashed) parton energy loss as compared to that of direct photons (dot-dashed) in central Au+Au collisions at $\sqrt{s} = 200$ GeV. $dE_q/dx = 1$ GeV/fm and mean free path $\lambda_q = 1$ fm are assumed. The contribution from soft particle production to the π_0 spectra is assumed to have a $A^{1.1}$ scaling.

in Fig. 2. Therefore, the shaded area in the figure (we only plotted for one case of energy loss) should be considered as one of the uncertainties of the ratio at low p_T associated with the interplay of contributions from soft and hard processes. One presumably can determine this dependence from future RHIC experimental data.

As we have stated earlier, the Cronin effect due to initial multiple parton scattering will introduce an uncertainty effect of 10–30% which can be narrowed down through a systematic study of $p+p$ and $p+A$ collisions. Since the concept of parton energy loss can only be applied to high E_T jets, it will in principle only affect the spectra at high p_T where contribution from soft production is negligible. At smaller values of $p_T < 3 \sim 4$ GeV/c where soft particle production becomes important, the connection between parton energy loss and the hadron spectra becomes unclear. In this region, the modification of the spectra is driven by parton and hadron thermalization. Since we approximate the spectra in this region by an effective A scaling of coherent or semicoherent particle production, the suppression factor we show in this paper can only be considered as semiquantitative. Furthermore, the spectra just above $p_T \sim 4$ GeV/c should also be sensitive to the energy dependence of the energy loss as we will show in the next section.

To further illustrate the effect of the parton energy loss in hadron spectrum we show in Fig. 3 the production rates of π^0 with (solid line) and without parton energy loss (dashed lines), together with the spectrum of direct photons (dot-dashed lines) at the RHIC energy. The upper curve for direct photons is a leading-order calculation multiplied by $K=2$ factor. The lower curve is the result of a next-to-leading order calculation [24] which also includes quark bremsstrahlung. Here we assumed the low- p_T soft particle spectra scales like $A^{1.1}$. Since we can neglect any electromagnetic interaction between the produced photon and the QCD medium, the photon spectrum will not be affected by the parton

energy loss. On the other hand, jet quenching due to parton energy loss can significantly reduce π^0 rate at large p_T . Therefore the change of γ/π^0 ratio at large p_T can also be an indication of parton energy loss. One can consider the contribution to direct photon production from bremsstrahlung as quark fragmentation into a photon, it should in principle also be affected by the quark energy loss inside the dense medium. Therefore, there is also some uncertainty (maximum factor of 2 if the $K=2$ factor completely comes from bremsstrahlung correction) to the estimated photon spectra at lower p_T where bremsstrahlung is more important.

IV. ENERGY AND A DEPENDENCE OF ENERGY LOSS

In recent theoretical studies of parton energy loss [5–7], it has been demonstrated that the so-called Landau-Pomeranchuk-Midgal (LPM) coherent effect can lead to interesting and sometimes nonintuitive results. Baier *et al.* have systematically studied these effects in detail [6,7]. They found that because of the modification of the radiation spectrum by the LPM coherence, the energy loss experienced by a fast parton propagating in an infinite large medium has a nontrivial energy dependence,

$$\frac{dE}{dx} \propto -N_c \alpha_s \sqrt{E \frac{\mu^2}{\lambda}} \ln \frac{E}{\lambda \mu^2} \quad (\text{for } L > L_{\text{cr}}), \quad (12)$$

where $N_c = 3$, E is parton's energy, μ^2 is the Debye screening mass for the effective parton scattering, λ is parton's mean free path in the medium, and $L_{\text{cr}} = \sqrt{\lambda E / \mu^2}$. For a more energetic parton traveling through a medium with finite length ($L < L_{\text{cr}}$), the final energy loss becomes almost independent of the parton energy and can be related to the total transverse momentum broadening acquired by the parton through multiple scattering,

$$\frac{dE}{dx} = -\frac{N_c \alpha_s}{8} \Delta p_T^2 = \frac{N_c \alpha_s}{8} \delta p_T^2 \frac{L}{\lambda}, \quad (13)$$

where δp_T^2 is the transverse momentum kick per scattering the parton acquires during the propagation. Therefore, the energy loss per unit distance, dE/dx , is proportional to the total length that the parton has traveled. Because of the unique coherence effect, the parton somehow knows the history of its propagation.

These are just two extreme cases of parton energy and the medium length. Since it involves two unknown parameters of the medium, it is difficult to determine which case is more realistic for the system of dense matter produced in heavy-ion collisions. We will instead study the phenomenological consequences of these two cases in the final single inclusive particle spectrum at large p_T .

Shown in Fig. 4 are the calculated suppression factors with an energy-dependent parton energy loss, $dE_q/dx = \sqrt{E}/5$ GeV and $dE_q/dx = \sqrt{E}/20$ GeV GeV/fm, respectively, for central Au+Au collisions at the RHIC energy. Comparing to Fig. 2 with a constant energy loss, suppression factors are flatter as functions of p_T . This is understandable because the energy loss for larger E_T jet will lose more energy in this scenario thus leading to a stronger suppression of high- p_T particles. As pointed out in Ref. [8], the most rel-

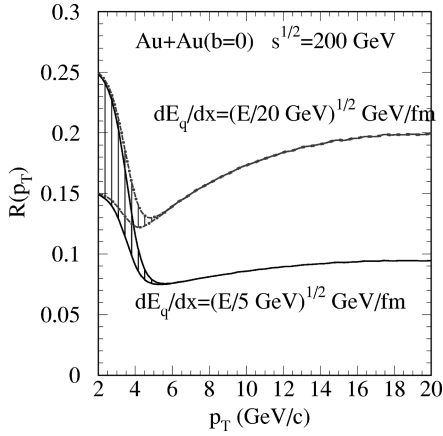


FIG. 4. The same as Fig. 2, except that an energy-dependent energy loss is assumed. The mean free path $\lambda_q = 1$ fm is used in the calculation.

evant quantity in the modification of the fragmentation functions is the parton energy loss ΔE_T relative to its original energy E_T . For a constant energy loss ΔE_T , the ratio $\Delta E_T/E_T$ becomes smaller for larger E_T , thus the suppression factor $R_{AA}(p_T)$ will increase with p_T . If the energy loss ΔE_T rises with the initial energy E_T , then the increase will be slower. Thus the slope of the ratio $R_{AA}(p_T)$ can provide us information about the energy dependence of the energy loss, as one can see from the comparison of Figs. 2 and 4.

To study the consequences of a parton energy loss dE/dx which increases with the distance L it travels, one can either vary the impact-parameter or the atomic mass of the projectile and target so as to change the size of the dense matter through which the leading partons have to propagate. Assuming a transverse size of the colliding nuclei which have a hard-sphere nuclear distribution, one can estimate that the averaged distance a produced jet has to travel through is $\langle L \rangle_A = 1.09A^{1/3}$, where one has to weight with the probability of jet production or the overlapping functions of AA collisions. In Fig. 5, we plot the suppression factor $R_{AA}(p_T)$ at a fixed $p_T = 10$ GeV/c for central $A+A$ collisions at the RHIC energy as a function of $A^{1/3}$, A the atomic masses of

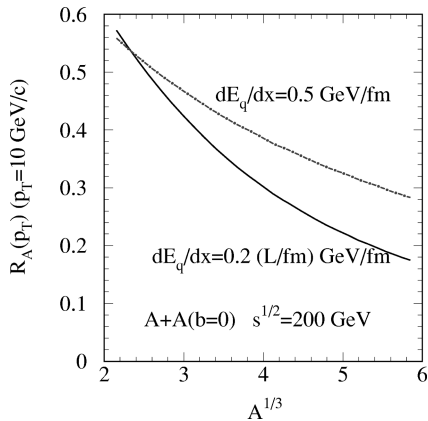


FIG. 5. The suppression factor for central $A+A$ collisions at $p_T = 10$ GeV/c, as a function of the system size, $A^{1/3}$, for a constant energy loss per unit distance length (dot-dashed line) and an energy loss which increases linearly with the length (solid line). The mean free path $\lambda_q = 1$ fm is used.

the projectile and target nuclei. The solid line is for an energy loss, $dE/dx = 0.2(L/\text{fm})$ GeV/fm, which is proportional to the total length traveled by the parton, and dot-dashed line is for a constant $dE/dx = 0.5$ GeV/fm. As the size of the system increases, a parton will lose more energy and thus will lead to increased suppression in both cases. For collisions of heavy nuclei ($A^{1/3} > 3$), the energy loss in the first case becomes larger than the second one and thus leads to more suppression. However, the functional form of the A dependence of the suppression factor in the two cases do not differ dramatically. It is therefore difficult to determine whether the energy loss per unit length is proportional to the total length simply from the A dependence of the suppression factor. It must require a model-dependent phenomenological study of the experimental data.

V. FLAVOR DEPENDENCE

Because of the non-Abelian coupling, gluons in QCD always have stronger interaction than quarks. The gluon density inside nucleons at small x is larger than quarks; the gluon-gluon scattering cross section is larger than the quark-quark; and a gluon jet produces more particles than a quark jet. For the same reason, a high-energy gluon will also lose more energy than a quark propagating through a dense medium. Theoretical calculations [5–7] all show that gluons lose twice as much energy as quarks. In this section we will discuss how to observe such difference in the final hadron spectrum.

By charge and other quantum number conservation, fragmentation functions of a gluon jet into particle and antiparticle will be identical, though it produces more particles than a quark jet and consequently its fragmentation functions are often softer than a quark's, as has been measured in the three-jet events of e^+e^- annihilation [25]. For example, an equal number of protons and antiprotons will be produced in the gluon fragmentation. On the other hand, an up or down quark is more likely to produce a leading proton than antiproton and vice versa for antiquarks. Since there will be more quark (up and down) jets produced than antiquark in nuclear collisions, one will find more protons than antiprotons, especially at large p_T since valence quarks are distributed at relatively large x (partons' fractional momenta of the nucleon), while gluons at small x . In other words, high p_T protons will have a smaller relative contribution from gluon jets than antiprotons. If gluon jets lose more energy than quark jets as we have assumed in this paper, one should then have different suppression factors for a proton and antiproton. Such flavor dependence should be most evident for heavy particles like nucleons and lambdas whose fragmentation functions from a valence quark are significantly harder (i.e., falls off more slowly at large z) and are very different from gluons and sea quarks. For light mesons like pions, the valence quark fragmentation functions are softer and are not much different from gluons and sea quarks. One then will not see much difference between the suppression factors for π^+ and π^- even though gluons and quarks have different energy loss.

Before we discuss the suppression factors, let us look at the flavor dependence of the spectra first. Plotted in Fig. 6 are π^-/π^+ ratios as functions of p_T in pp , central Au+Au

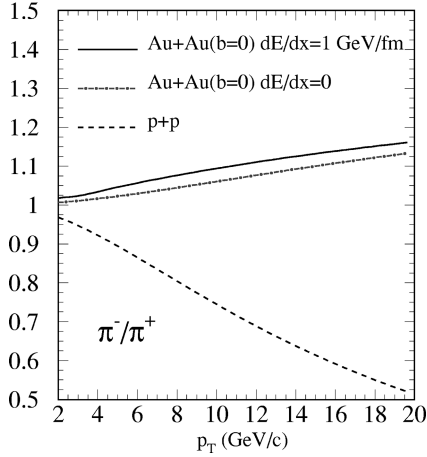


FIG. 6. The ratio of π^- to π^+ spectra as functions of p_T in pp (dashed), central Au+Au collisions at $\sqrt{s}=200A$ GeV without energy loss (dot-dashed) and with energy loss of $dE_q/dx = 1$ GeV/fm (the mean free path $\lambda_q = 1$ fm).

collisions with and without energy loss at $\sqrt{s}=200A$ GeV. Because gluon-quark scattering dominates in this p_T region at the RHIC energy and there are twice as many valence u quarks than d quarks in pp collisions, this ratio decreases with p_T (dashed line) and should saturate at about 0.5 (valence d to u quark ratio in a proton) at very high p_T where only valence quarks contribute to pion production. At low p_T where contributions from sea quarks and gluons become more important the ratio is then close to one. This is a clear prediction of QCD parton model and has been verified by experiments some years ago [26]. In Au+Au collisions, however, there are slightly more valence d quarks than u quarks since the nuclei are slightly neutron rich. As we see in the figure, the π^-/π^+ ratio (dot-dashed line) then increases with p_T and approaches a value of about 1.14 which is the valence d to u quark ratio in a Au nucleus. The reason why the ratio is different from the limit of d/u ratio is because of finite contributions from sea quarks and gluons. If gluons lose more energy than quarks, the contribution to high- p_T pion production from gluons will be reduced relative to quarks. Therefore, the π^-/π^+ ratio will be higher than the case of no difference in energy loss between quarks and gluons (or no energy loss) or become closer in value to the d/u ratio, as we see in the figure (solid line). However, the change due to the parton energy loss is very small because the contributions to pion production from gluons is relatively much smaller than quarks.

The situation for protons and antiprotons is different. From parton distributions in a proton we know that gluon to quark density ratio $f_{g/p}(x, Q^2)/f_{q/p}(x, Q^2)$ decreases with $x = 2E_T/\sqrt{s}$, where E_T is the transverse momentum of the produced jet. Consequently the ratio of gluon to quark jet production cross section always decreases with E_T . Since most of antiprotons come from gluons while protons come from both valence quark and gluon fragmentation, the ratio of antiproton to proton production cross section should also decrease with their p_T , as our calculation shows in Fig. 7 for pp collisions (dashed line) at $\sqrt{s}=200$ GeV. At small p_T gluon and quark jet cross sections become comparable, so the ratio \bar{p}/p should increase. But it will always be smaller

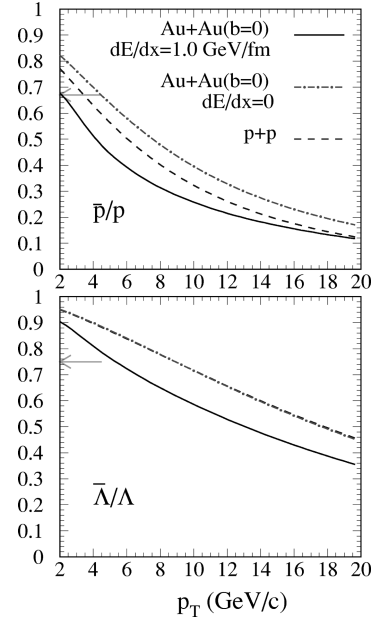


FIG. 7. The ratio of \bar{p} to p (upper panel) and $\bar{\Lambda}$ to Λ (lower panel) spectra as functions of p_T in pp (dashed), central Au+Au collisions at $\sqrt{s}=200A$ GeV without energy loss (dot-dashed) and with energy loss of $dE_q/dx=1$ GeV/fm (solid) (the mean free path $\lambda_q=1$ fm). Gluons are assumed to lose twice as much energy as quarks. The arrows indicate the ratio at low $p_T < 1$ GeV/c from HIJING/BJ estimate (with the baryon junction model of baryon stopping).

than 1 because there will always be more protons than anti-protons in nucleon or nuclear collisions due to baryon number conservation (and finite net baryon production in the central region even from perturbative QCD calculation).

The dot-dashed line in Fig. 7 is the \bar{p}/p ratio in central Au+Au collisions without parton energy loss at the RHIC energy. Since Au nuclei are slightly neutron rich, one should have less proton production per nucleon from valence quark fragmentation than pp collisions. Since gluon jet production does not change from pp to Au+Au, the ratio \bar{p}/p in Au+Au (without energy loss) is then a little larger than in pp collisions. If there is parton energy loss and gluons lose more energy than quarks, then as we have argued that \bar{p}/p ratio should become smaller than without energy loss (or gluons and quarks have the same energy loss), as shown in the figure as the solid line. The result and argument is the same for $\bar{\Lambda}/\Lambda$ ratio as also shown in the lower panel of Fig. 7. To further illustrate this point, we plot in Fig. 8 the particle suppression factors for the proton, antiproton, lambda, and antilambda as functions of p_T . Because of the increased energy loss for gluons over quarks, the suppression factors for antiprotons and antilambdas is then smaller than protons and lambdas. This could be easily verified if one can identify these particles at high p_T in experiments.

In the calculation of high- p_T baryon spectra in Figs. 7 and 8 one has to use parametrized fragmentation functions for baryons similarly to these of mesons [12,13]. Though baryon production from jet fragmentation in e^+e^- and e^-p collisions has been studied [27], we could not find any parametrized form including the Q^2 evolution. Since the Lund model has been proven to reproduce the experimental data

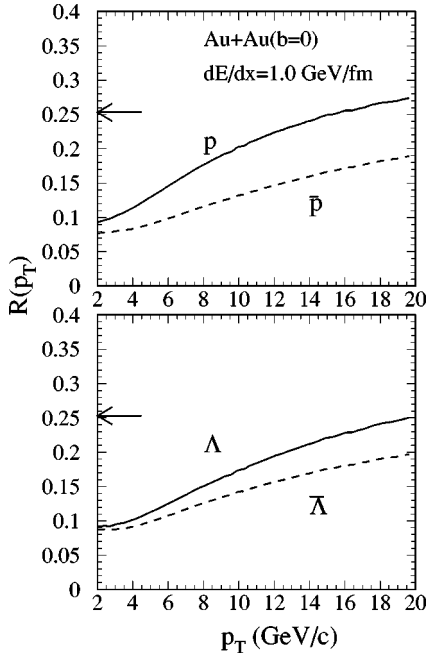


FIG. 8. Particle suppression factors for p , Λ (solid) and \bar{p} , $\bar{\Lambda}$ (dashed) as functions of p_T in central Au+Au collisions at $\sqrt{s} = 200A$ GeV with energy loss of $dE_q/dx = 1$ GeV/fm and mean free path $\lambda_q = 1$ fm. Gluons are assumed to lose twice as much energy as quarks. The arrows indicate the suppression factors at low $p_T < 1$ GeV/c if the soft particle production is assumed to have an $A^{1.1}$ scaling.

well, here we use the baryon fragmentation functions parametrized from the Monte Carlo simulation of Lund model (JETSET) [29]. The parametrizations are given in the Appendix.

In the calculation of the particle ratio in Figs. 6 and 7 and particle suppression factors in Fig. 8, we included only contributions from perturbative hard processes. As we have discussed before there will also be particle production from nonperturbative processes. These soft particle productions, which are dominant at low p_T , are not likely to change the π^-/π^+ ratio much. However, it might change the \bar{p}/p and $\bar{\Lambda}/\Lambda$ ratio, as recent heavy-ion experiments show [28] that there is significantly more baryon stopping than either pQCD calculation or a simple Lund string model of nuclear collisions. There are many models of nonperturbative baryon stopping in nuclear collisions [30,31]. To take into account this nonperturbative baryon stopping, a baryon junction model [32] has been implemented into the original HIJING model to describe the observed baryon stopping at SPS energy [33]. This version of the HIJING (or HIJING/BJ) model at the RHIC energy gives a ratio of $\bar{p}/p = 0.67$ and $\bar{\Lambda}/\Lambda = 0.75$. These values should serve as an estimate of the particle ratio at small $p_T < 1$ GeV/c, as indicated by the arrows in Fig. 7. This then gives us an upper bound of the uncertainty for the ratio at around $p_T \sim 2$ GeV/c, depending on the interplay between perturbative and nonperturbative contributions. Similarly, the suppression factors at low p_T also depend on the A scaling of low- p_T particle production. If we assume an $A^{1.1}$ scaling like we did for all charged particles, then the suppression factors at low $p_T < 1$ GeV/c should be as indicated by the arrows in Fig. 8. Since contributions from

the stopped baryon scale like A , the low p_T limit for baryons will then be smaller than antibaryons. This is an upper bound of the uncertainty one should bear in mind at intermediate p_T . At large p_T these uncertainties will become very small.

Similarly as we have discussed in the previous sections, the particle ratio and suppression factors will all depend on the other parameters of the energy loss and its energy and A dependence. But these will not change the qualitative feature of the flavor dependence of the particle suppression due to different energy loss suffered by gluons and quarks. Because of finite net baryon density in the central region, the baryon and antibaryon absorption in the hadronic phase will be slightly different which might also give rise to different suppression factors for baryons and antibaryons. A detailed study of this effect is out of the scope of this paper. However, at very large p_T , the physical baryons might only be formed outside the dense region of hadronic matter. Before then, the color neutral object might have very a small cross section with other hadrons which have already been formed. Thus the effect of baryon annihilation might be very small at large p_T . The study of the data for high p_T particle production in Pb+Pb collisions at the SPS energy support this scenario [18].

VI. CONCLUSIONS

A systematic study of the effects of parton energy loss in dense matter on the high p_T hadron spectra in high-energy heavy-ion collisions has been carried out in this paper. We found the hadron spectra at high p_T is quite sensitive to how the large- E_T partons interact with the dense medium and lose their energy before they fragment into hadrons, leading to the suppression of high- p_T particles. The suppression factor as a function of p_T is also sensitive to the energy dependence of the parton energy loss. Even though the nonlinear length dependence of the energy loss as suggested by a recent theoretical study [7] leads to stronger suppression, one cannot unambiguously determine the nonlinearity by varying the system size. We also studied the flavor dependence of the particle spectra and the suppression factor and found that it is a good probe of the energy loss, especially the difference between the energy loss of a gluon and a quark.

Because of our lack of a quantitative understanding of energy loss of the produced high E_T parton jets inside the dense matter in heavy-ion collisions, our phenomenological study in this paper can only be qualitative. But such a qualitative study is essential to establish whether there is parton energy loss at all in heavy-ion collisions and thus whether there is such an initial stage in the collisions when the produced dense matter is equilibrating. The analysis we proposed in this paper, which is also somewhat model dependent, can at least provide information about the average total energy loss the parton could have suffered during its interaction with the medium. Anything beyond that will require our knowledge of the dynamical evolution of the system. Even toward such a modest goal, there is still one final hurdle to overcome, i.e., final-state interactions between leading hadrons of a jet and the soft particles in the hadronic matter. Such an issue is very important to the determination of whether the high- p_T particle suppression, if any, is indeed caused by parton energy loss in the initial stage of a dense-

partonic matter. Since the formation time of a large- p_T particle is longer than the soft ones, a large- p_T particle might be physically formed outside the dense region of the hadronic phase. Before then, it is in the form of a color dipole which might have very small interaction cross section with other hadrons. Therefore, the hadronic phase of the dense matter might have a very small effect on the high- p_T particle spectra. One could address this issue in heavy-ion collisions at the SPS energies [18], where one would at least expect that a dense hadronic matter has been formed.

ACKNOWLEDGMENTS

The author would like to thank S. Vance for providing the estimate of \bar{p}/p and $\bar{\Lambda}/\Lambda$ ratios from HIJING/BJ calculations. This work was supported by the Director, Office of Energy Research, Office of High Energy and Nuclear Physics, Divisions of Nuclear Physics, of the U.S. Department of Energy under Contract Nos. DE-AC03-76SF00098 and DE-FG03-93ER40792. The author wishes to thank the Institute for Nuclear Theory for kind hospitality during his stay when this work was written.

APPENDIX

In this appendix we list the baryon fragmentation functions parametrized from the results of Lund JETSET Monte Carlo program [29]. We simulate the fragmentation of a $q\bar{q}$ or a two-gluon system with invariant mass $W=2Q$, and then parametrize the particle distributions along one direction of the jet axes as functions of $z=E_h/Q$. We choose the form of the parametrization as [12]

$$D_a^h(z, Q) = \langle n_h(Q) \rangle N z^\alpha (1-z)^\beta (1+z)^\gamma, \quad (A1)$$

if the parton a is a gluon or sea quark, and

$$D_a^h(z, Q) = \langle n_h(Q) \rangle [N_1 z^{\alpha_1} (1-z)^{\beta_1} (1+z)^{\gamma_1} + N_2 z^{\alpha_2} (1-z)^{\beta_2}], \quad (A2)$$

if the parton is a valence quark of the hadron h . The fragmentation functions are normalized as $\int_0^1 dz D_a^h(z, Q) = \langle n_h(Q) \rangle$. For a rough approximation which is enough for a qualitative study in this paper, we neglect the change of the shape of distributions according to the QCD evolution and attribute the energy dependence to the average multiplicity $\langle n_h(Q) \rangle$, which are parametrized as

$$\langle n_h(Q) \rangle = a + bs + cs^2, \quad (A3)$$

$$s = \ln \frac{\ln(Q^2/\Lambda_{\text{QCD}}^2)}{\ln(Q_0^2/\Lambda_{\text{QCD}}^2)},$$

where we choose $Q_0 = 1$ GeV.

(1) Gluons:

$$D_g^n = D_g^n, \quad N = 3.814, \quad \alpha = -0.187, \quad \beta = 3.660, \quad \gamma = -2.231, \\ a = 0.061, \quad b = 0.147, \quad c = 0.155. \quad (A4)$$

$$D_g^p = D_g^{\bar{p}}$$

$$N = 3.814 \quad \alpha = -0.187, \quad \beta = 3.660, \quad \gamma = -2.231, \\ a = 0.047, \quad b = 0.161, \quad c = 0.133. \quad (A5)$$

$$D_g^\Lambda = D_g^{\bar{\Lambda}}$$

$$N = 3.378, \quad \alpha = -0.166, \quad \beta = 4.394, \quad \gamma = 0.105, \\ a = 0.0215, \quad b = 0.0454, \quad c = 0.0568. \quad (A6)$$

(2) d quarks:

$$D_d^n$$

$$N_1 = 0.002, \quad \alpha_1 = -2.303, \quad \beta_1 = 6.461, \quad \gamma_1 = 20.225, \\ N_2 = 1.671, \quad \alpha_2 = 0.699, \quad \beta_2 = 1.311, \quad (A7) \\ a = 0.0966, \quad b = 0.0419, \quad c = 0.1045.$$

$$D_d^p$$

$$N_1 = 0.005, \quad \alpha_1 = -2.246, \quad \beta_1 = 4.464, \quad \gamma_1 = -2.141, \\ N_2 = 1.377, \quad \alpha_2 = -0.252, \quad \beta_2 = 2.142, \quad (A8) \\ a = 0.0392, \quad b = 0.0356, \quad c = 0.0906.$$

$$D_d^\Lambda$$

$$N = 0.230, \quad \alpha = -1.027, \quad \beta = 1.962, \quad \gamma = 3.037, \\ a = 0.0098, \quad b = 0.0269, \quad c = 0.0250. \quad (A9)$$

$$D_d^{\bar{n}}$$

$$N = 0.318, \quad \alpha = -0.989, \quad \beta = 4.956, \quad \gamma = 5.186, \\ a = 0.0104, \quad b = 0.0867, \quad c = 0.0743. \quad (A10)$$

$$D_d^{\bar{p}}$$

$$N = 0.318, \quad \alpha = -0.989, \quad \beta = 4.956, \quad \gamma = 5.186, \\ a = 0.0124, \quad b = 0.0676, \quad c = 0.0760. \quad (A11)$$

$$D_d^{\bar{\Lambda}}$$

$$N = 0.318, \quad \alpha = -0.989, \quad \beta = 4.956, \quad \gamma = 5.186, \\ a = 0.0033, \quad b = 0.0232, \quad c = 0.0265. \quad (A12)$$

(3) u quarks:

By isospin symmetry: $D_u^{p(\bar{p})} = D_d^{n(\bar{n})}$, $D_u^{n(\bar{n})} = D_d^{p(\bar{p})}$, $D_u^{\Lambda(\bar{\Lambda})} = D_d^{\Lambda(\bar{\Lambda})}$.

(4) s quarks:

$$D_s^\Lambda$$

$$N_1 = 9.55 \times 10^{-5}, \quad \alpha_1 = -3.09, \quad \beta_1 = 8.344, \quad \gamma_1 = 31.74, \\ N_2 = 11.880, \quad \alpha_2 = 2.790, \quad \beta_2 = 1.680, \quad (A13) \\ a = 0.0706, \quad b = 0.0546, \quad c = 0.0113.$$

$$D_s^n$$

$$N=0.254, \quad \alpha=-1.0123, \quad \beta=3.506, \quad \gamma=4.385,$$

$$a=0.0362, \quad b=0.0228, \quad c=0.1087. \quad (\text{A14})$$

$$D_s^p$$

$$N=0.421, \quad \alpha=-0.867, \quad \beta=3.985, \quad \gamma=3.577,$$

$$a=0.0326, \quad b=0.0149, \quad c=0.1060. \quad (\text{A15})$$

$$D_s^{\bar{n}}$$

$$N=0.410, \quad \alpha=-0.931, \quad \beta=5.549, \quad \gamma=4.807,$$

$$a=0.0123, \quad b=0.0631, \quad c=0.0869. \quad (\text{A16})$$

$$D_s^{\bar{p}}$$

$$N=0.410, \quad \alpha=-0.931, \quad \beta=5.549, \quad \gamma=4.807,$$

$$a=0.0135, \quad b=0.0456, \quad c=0.0935. \quad (\text{A17})$$

$$D_s^{\bar{\Lambda}}$$

$$N=0.238, \quad \alpha=-1.060, \quad \beta=7.141, \quad \gamma=9.106,$$

$$a=0.00197, \quad b=0.0331, \quad c=0.0174. \quad (\text{A18})$$

(5) Antiquarks: By symmetry of charge conjugate: $D_q^{\bar{B}}=D_q^B$
 $D_q^{\bar{B}}=D_q^B$.

-
- [1] K. Geiger, Phys. Rep. **256**, 237 (1995).
 [2] X.-N. Wang, Phys. Rep. **280**, 287 (1997).
 [3] B. Müller, Rep. Prog. Phys. **58**, 611 (1995).
 [4] K. Eskola, CERN-TH-97-220, 1997, hep-ph/9705027.
 [5] M. Gyulassy and X.-N. Wang, Nucl. Phys. **B420**, 583 (1994); X.-N. Wang, M. Gyulassy, and M. Plümer, Phys. Rev. D **51**, 3436 (1995).
 [6] R. Baier, Yu. L. Dokshitzer, S. Peigné, and D. Schiff, Phys. Lett. B **345**, 277 (1995).
 [7] R. Baier, Yu. L. Dokshitzer, A. Mueller, S. Peigné, and D. Schiff, hep-ph/9608322.
 [8] X.-N. Wang, Z. Huang, and I. Sarcevic, Phys. Rev. Lett. **77**, 231 (1996).
 [9] X.-N. Wang and Z. Huang, Phys. Rev. C **55**, 3047 (1997).
 [10] X.-N. Wang and M. Gyulassy, Phys. Rev. Lett. **68**, 1480 (1992).
 [11] P. Mättig, Phys. Rep. **177**, 141 (1989).
 [12] J. Binnewies, B. A. Kniehl, and G. Kramer, Z. Phys. C **65**, 471 (1995).
 [13] Kaon fragmentation functions are adopted from J. Binnewies, B. A. Kniehl, and G. Krame, Phys. Rev. D **52**, 4947 (1995).
 [14] R. Baier, Yu. L. Dokshitzer, A. H. Mueller, and D. Schiff, hep-ph/9803473.
 [15] J. F. Owens, Rev. Mod. Phys. **59**, 465 (1987).
 [16] K. J. Eskola and X.-N. Wang, Int. J. Mod. Phys. A **10**, 3071 (1995).
 [17] X.-N. Wang and M. Gyulassy, Phys. Rev. D **44**, 3501 (1991); Comput. Phys. Commun. **83**, 307 (1994).
 [18] X.-N. Wang, Phys. Rev. Lett. (to be published).
 [19] A. D. Martin, W. J. Stirling, and R. G. Roberts, Phys. Lett. B **306**, 145 (1993).
 [20] British-Scandinavian Collaboration, B. Alper *et al.*, Nucl. Phys. **B87**, 19 (1975).
 [21] UA1 Collaboration, C. Albajar *et al.*, Nucl. Phys. **B335**, 261 (1990).
 [22] F. Abe *et al.*, Phys. Rev. Lett. **61**, 1819 (1988).
 [23] UA1 Collaboration, G. Arnison *et al.*, Phys. Lett. B **172**, 461 (1986); C. Albajar *et al.*, Nucl. Phys. **B309**, 405 (1988).
 [24] J. Cleymans, E. Quack, K. Redlich, and D. K. Sirvastava, Int. J. Mod. Phys. A **10**, 2941 (1995).
 [25] For example, DELPHI Collaboration, P. Abreu *et al.*, Z. Phys. C **70**, 179 (1996).
 [26] D. Antreasyan *et al.*, Phys. Rev. D **19**, 764 (1979); D. Drijard *et al.*, Nucl. Phys. **B208**, 1 (1982).
 [27] D. Indumathi, H. S. Mani, and A. Rastogi, hep-ph/9802324, 1998, and references therein.
 [28] See, proceedings of Quark Matter '97, Tsukuba, 1997.
 [29] B. Andersson, G. Gustafson, G. Ingelman, and T. Sjöstrand, Phys. Rep. **97**, 31 (1983).
 [30] A. Capella, J. Phys. G **23**, 1979 (1997).
 [31] H. Stöcker *et al.*, Nucl. Phys. **A590**, 217 (1995); Proceedings of Quark Matter '95, Monterey, 1995.
 [32] D. Kharzeev, Phys. Lett. B **378**, 238 (1996).
 [33] S. Vance, M. Gyulassy, and X.-N. Wang, Proceedings of Quark Matter '97, Tsukuba, Japan, 1997.